Biochemical and Biophysical Research Communications 622 (2022) 30–36

Contents lists available at ScienceDirect

Biochemical and Biophysical Research Communications

journal homepage: www.elsevier.com/locate/ybbrc

Study of the influence of hyperglycemia on the abundance of amino acids, fatty acids, and selected lipids in extracellular vesicles using TOF-SIMS

Magdalena E. Marzec [a, b], Carina Rząca [a, b], Paweł Moskal [b, c], Ewa Ł. Stępień [a, b, *]

[a] Department of Medical Physics, M. Smoluchowski Institute of Physics, Faculty of Physics, Astronomy and Applied Computer Science, Jagiellonian University, Lojasiewicza 11 St, 30-348, Krakow, Poland
[b] Center for Theranostics, Jagiellonian University, Kopernika 40 St, 31-501, Krakow, Poland
[c] Department of Experimental Particle Physics and Applications, M. Smoluchowski Institute of Physics, Faculty of Physics, Astronomy and Applied Computer Science, Jagiellonian University, Lojasiewicza 11 St, 30-348, Krakow, Poland

ARTICLE INFO

Article history:
Received 24 June 2022
Accepted 6 July 2022
Available online 9 July 2022

Keywords:
ToF-SIMS
Lipids
Ectosomes
Exosomes
Hyperglycemia

ABSTRACT

Time-of-flight secondary ion mass spectrometry (TOF-SIMS) with the Bi_3^+ liquid metal ion gun was used to investigate the content of lipids and amino acids (AAs) in extracellular vesicles (EVs). We induced metabolic changes in human pancreatic β-cells by stimulation with high glucose concentrations (35 mM) and tested the hypothesis of hyperglycemia (HG) has a detrimental effect on lipids and AAs in released EV subpopulations: ectosomes and exosomes. As a result of HG treatment, selected fatty acids (FAs) such as arachidonic, myristic and palmitic acids, changed their abundance in ectosomes and exosomes. Also, intensities of the characteristic peaks for cholesterol (*m/z* 95.09; 147.07; 161.11; 369.45) along with the molecular ion *m/z* 386.37 [$C_{27}H_{46}O^+$] under HG conditions, both for ectosomes and exosomes, have changed significantly. Comparative analysis of HG EVs and normoglycemic (NG) ones showed statistically significant differences in the signal intensities of four AAs: valine (*m/z* 72.08 and 83.05), isoleucine (*m/z* 86.10), phenylalanine (*m/z* 120.08 and 132.05) and tyrosine (*m/z* 107.05 and 136.09). We confirmed that ToF-SIMS is a useful technique to study selected AAs and lipid profiles in various EV subpopulations. Our study is the first demonstration of changes in FAs and AAs in exosomes and ectosomes derived from β-cells under the influence of HG.

1. Introduction

Lipids are ubiquitous molecules that are involved in a myriad of cellular processes. Due to their structure, lipids are sensitive to each preparation step, therefore the possibility of testing them in their native state, without the extraction from biological material, is exceptionally promising [1]. In the case of Time of Flight – Secondary Ion Mass Spectrometry (ToF-SIMS), there is no need to perform such preparations or labelling, which allows the structure to be examined in a semi-native state [2]. Thanks to these advantages, the ToF-SIMS technique has become a valuable tool in biology and medicine for the localization of elements, molecules, radiolabeled compounds and lipids in cells and tissues in the mass range up to *m/z* 1000 [3,4].

In our study, we analyzed biological samples consisting of different extracellular vesicles (EVs) secreted by human pancreatic β-cells under high and normal glucose concentrations. EVs are spherical, submicron cell structures surrounded by a protein-lipid membrane, released by almost all animal and human cells. They have several physical and biological properties that are important for cell-to-cell communication [5]. The basic classification of EVs distinguishes three subpopulations: exosomes derived from endosomes (50–150 nm), cell ectosomes (100–1000 nm) and apoptotic bodies (1000–5000 nm). Specific features of these EV subgroups have been proposed and well defined, but there is still an

Abbreviations: AAs, aminoacids; EVs, extracellular vesicles; FAs, fatty acids; FBS, foetal bovine serum; GPC, glycerophosphocholine; HG, hyperglycemia; NG, normoglycemic; PC, phosphatidylcholine; PE, phosphatidylethanolamine; PKC, protein kinase C; ROS, reactive oxygen species; T2D, type 2 diabetes; TOF-SIMS, Time-of-flight secondary ion mass spectrometry; TRPS, tunable resistive pulse sensing.

* Corresponding author. Department of Medical Physics M. Smoluchowski Institute of Physics Faculty of Physics, Astronomy and Applied Computer Science, Lojasiewicza 11 St, 30-348, Krakow, Poland.
E-mail address: e.stepien@uj.edu.pl (E.Ł. Stępień).

https://doi.org/10.1016/j.bbrc.2022.07.020

unmet need for universal markers to differentiate these subpopulations [6,7].

Recent studies have shown that EVs are new bio-mediators of type 2 diabetes (T2D) and cardiovascular disease [8,9]. An example may be the work suggesting that hyperglycemia (HG) stimulates increased EVs secretion, as elevated levels of endothelial EVs (microparticles) have been reported in people with pre-diabetes compared to people with normal glucose tolerance [10]. *In vitro* studies have shown, that HG increases EV release compared to normal glucose (NG) concentrations [9,11]. However, there are few experimental data on the effect of high glucose concentrations on vesicular transport in the insulin-secreting cells and pancreatic β-cells [12,13].

We proposed here the use of ToF-SIMS to evaluate the differences in the molecular composition of exosomes, ectosomes and a mixture of these two populations. The tested EVs were derived from human pancreatic β-cells cultured in NG and HG conditions [7].

2. Materials and methods

2.1. Human-cell line culture

The human pancreatic β-cell line (1.1B4) was maintained in RPMI 1640 medium supplemented with 10% foetal bovine serum (FBS), 1% 200 mM L-glutamine and antibiotics - 100 μg/mL streptomycin and 100 units/mL penicillin. Cells were grown in a monolayer at 37 °C and a humidified atmosphere of 5% CO_2 until reaching about 80% of confluence [12,14]. Half of the dishes were cultured under NG conditions (11 mM D-glucose), while the second half was grown under long-term (3 passages) HG conditions (35 mM D-glucose). For further analyses, sub-confluent cells were maintained for 24 h in FBS-free RPMI 1640 medium and the conditioned medium with EVs was collected.

2.2. Isolation of EV subpopulations

The harvested conditioned media were centrifuged at 400×*g* for 10 min and 3 100×*g* for 25 min (Eppendorf 5424R, Germany) to remove cell fragments and debris. Then supernatants in a volume of 300 mL were concentrated using the 1000 kDa molecular weight cut-off dialysis cellulose membranes (Spectra/Por Biotech) at low pressure (−0.3 Bar) to obtain 1 ml of the EVs sample [7]. In the next step, the concentrated sample was centrifuged at 7 000×*g* for 20 min to remove apoptotic bodies. The pellet was analyzed and the supernatant was further divided into two tubes which were then centrifuged to separate the different EV fractions: (1) mixed fraction of EVs, (2) ectosomes fraction and (3) exosomes fraction.

(1) **Mixed EVs**: the sample was ultracentrifuged for 1.5 h at 150 000×*g* and 4 °C and suspended in 50 μL of PBS.
(2) **Ectosomes**: the sample was firstly centrifugated for 20 min at 18 000×*g* and 4 °C, the obtained pellet was washed with 1 mL of PBS and centrifugated again under the same conditions.
(3) **Exosomes**: the supernatant of fraction (2) was collected and ultracentrifuged for 1.5 h at 150 000×*g* and 4 °C, next suspended in 50 μL of PBS.

2.3. Determination of size distribution and concentration

The size distribution and EVs concentration derived from pancreatic β-cells cultured in NG and HG conditions were determined by the tunable resistive pulse sensing (TRPS) technique (qNano; Izon, Christchurch, New Zealand). The calibration was performed using CPC200 polystyrene beads suspended in PBS, with an average size of 200 nm and a raw concentration of 7×10^{11} particles/mL. The particle number was counted using NP150 and NP200 nanopores membranes stretched to 47 mm. The data were analyzed using the Izon Control Suite software (*ver.* 3.4).

2.4. Sample preparation

Before EVs deposition, the silicon substrates (1×1 cm^2) were cleaned in a freshly prepared Piranha solution (H_2SO_4: H_2O_2 = 3:1, v/v) for 60 s at 40 °C, immediately rinsed with ultrapure water for three times and then dried with nitrogen. The volume of 30 μL of each sample at the concentration of EVs adjusted to 3×10^9 particles/mL was applied to the prepared substrates and allowed to adhere during the 1-h incubation. Prior to the measurement, samples were washed with PBS buffer, rinsed with ultrapure water and dried in a stream of N_2.

2.5. ToF-SIMS measurements

All experiments were performed using the ToF-SIMS 5 spectrometer (ION-ToF GmbH, Münster, Germany) with a Bi_3^+ (30 keV) liquid metal ion gun, as a primary ion source. Spectra were recorded in the mass range of 0–900 Da with a mass resolution of 8300 @ *m/z* 600 (FWHM). The analysis of the amino acids and lipids composition were performed in the static spectrometer mode with a current equal to 0.75 pA and the total dose density was 1.88×10^{11}/cm^2. Measurements were carried out at the same time and under the same conditions with a single sample holder, which allows for comparative data analysis.

Two biological replicates were conducted for individual EVs sample, and three different places on the surface each sample with the size of 150×150 μm^2 for positive ions were examined. Finally, six mass spectra were obtained from a given area for each sample (1), (2), (3). Every single spectrum was calibrated using signals for positive ions: H^+, H_2^+, CH^+, CH_2^+, CH_3^+ and $C_3H_2^+$. Raw and analyzed data from these experiments are available at the Jagiellonian University Repository [15].

A statistical analysis was performed, in which the mean values and standard deviations of the intensity for the selected peaks for each group of samples were calculated. The significance of differences between the mean values for the groups was determined based on Tukey's test and the one-way ANOVA. The significance level for the tests was $p \leq 0.05$. The SurfaceLab *ver.* 7.2 for data analysis was used, enabling the re-edition of performed measurements. The academic version of the OriginPro software (*ver.* 9.8.0.200, 2020b) was used to perform one-way ANOVA and all plotted graphs.

3. Results and discussion

3.1. Size and enumeration of EVs by the TRPS technique

Based on our results (Fig. 1), we confirmed that two general EV subpopulations (exosomes and ectosoemes) were isolated showing the mean exosome diameter at 94 nm and around 170 nm for ectosomes, the similar diameter was measured for the mixed population of EVs. These results showed that β-cells produce EVs smaller in size compared to *e.g.* human endothelial cells subject to similar conditions [16]. In fact, not only centrifugation forces and rotor geometry influence EVs sedimentation. Environment conditions such as solvent density (ρ_{solv}) and viscosity (η) are the adjustable factors for controlling EV isolation (**Suppl. File 1**) [17].

To characterize the EV release, we determined their number and

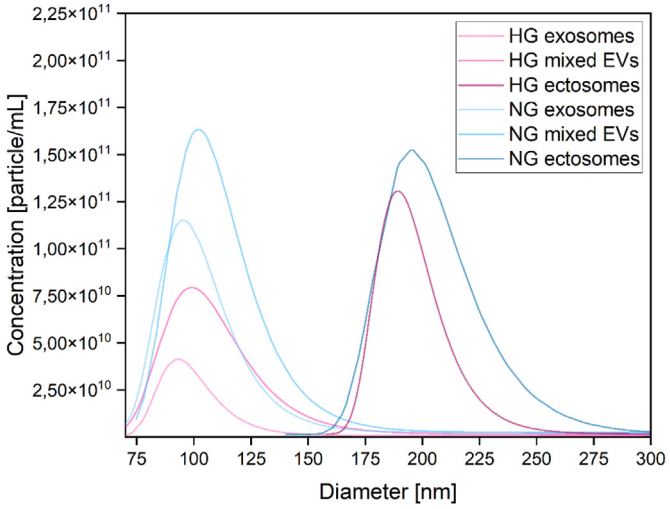

Fig. 1. Size distribution and raw concentration of EVs isolated from pancreatic β-cells conditioned media. Correlational analysis: *statistically significant with p-value <0.05.

observed their increase under NG conditions, for both ectosome and mixed EV fractions. The concentration for NG exosomes is the uncertainty of values for the other two groups (Fig. 1).

3.2. ToF-SIMS comparative analysis

3.2.1. Amino acids

In our analysis were distinguished five amino acids (AAs), including valine, leucine, isoleucine, phenylalanine and tyrosine, which are predictors of T2D (Fig. 2 A, B, C) [18,19].

In the fraction (1), containing a mixture of all EVs, we noticed that only one ion, characteristic for valine [$C_4H_8N^+$], with a mass of m/z 72.08, changed significantly and higher intensity was observed for EVs isolated from HG cells [20]. In the fraction (2), containing ectosomes, statistically significant changes occurred for most of the characteristic peaks, except one for valine (m/z 83.05, [$C_4H_5N_2^+$]). In this fraction, higher intensities in NG were observed for two peaks: valine [$C_4H_8N^+$] and isoleucine (m/z 86.10, [$C_4H_6NO^+$]) [20]. The most significant differences were observed in the fraction (3), containing exosomes, showing significantly higher intensities for valine, isoleucine, phenylalanine (m/z 120.08, [$C_7H_7O^+$] and 132.05, [$C_5H_{11}N_4^+$]) and tyrosine (m/z 107.05, [$C_4H_{10}N_3^+$] and 136.09, [$C_9H_8N^+$]) in exosomes derived from cells cultured in HG [20,21].

Several AAs are known to be associated with insulin resistance and increased risk of T2D [22,23]. Our study is the first to show that the relationship between glucose and AA levels in HG can be reflected in EVs composition, particularly in exosomes subpopulation (Fig. 2).

3.2.2. Fatty acids

Fatty acids (FAs) exist in two forms: “free” form as free fatty acids (FFA) or FAs as components of fats [24]. There are many evidences of a relationship between elevated glucose levels and FFA levels [25]. These stages may be elevated in diabetes due to the accelerated mobilization of fat stores, which corresponds to the lack of adipocytes response to the inhibitory effect of insulin on lipolysis [25,26].

In contrast, after splitting fraction (1) to fraction of ectosomes and exosomes, we observed that several important FAs such as arachidonic (20:4 ω-6), myristic (14:0) and palmitic (18:0) acids changed their abundance in different glucose concentrations (Fig. 2 (D, E, F)). We observed that the lowest masses, referring to the arachidonic, myristic and palmitic acid fragments, for the EVs mixture did not expressed significant differences between HG and NG. In the group of ectosomes (Fig. 2 E), there were statistically significant differences, where higher intensities were observed for NG ectosomes. The same association occurred in the third group, for exosomes. For the next mass, with the formula [$C_{14}H_{29}O_2^+$], which corresponds to the myristic acid molecular ion, for the fractions (1) and (2), no statistical differences were found, while for exosomes (fraction (3)), it can be noticed that the intensity is significantly higher for HG. It was shown, that glucose preferentially increased C16:0-containing, di-saturated DAG species which indicated TAG hydrolysis after glucose stimulation in β-cells [27]. In our study, we observed a lower abundance of palmitic acid fragments in HG exosomes (Fig. 2 E), which may reflect the turnover of membrane lipid, and in particular arachidonic-containing phospholipids and diacylglycerols, in glucose-stimulated β-cells. Next, we observed a lower intensity for 20:4 ω-6 in EVs isolated from β-cells exposed to chronic and extensive HG, as shown in β-cells [28].

3.2.3. Sterols and prenols

To complete the HG study along with metabolic changes in EVs derived from human β-cells we performed the SIMS analysis of sterols (Fig. 3 A, B, C).

Comparative analysis in the sterol lipid group showed changes in the mean, normalized intensities for the characteristic masses of three EV fractions. Five masses were included in the analysis, four cholesterol fragments: m/z: 95.09 [$C_7H_{11}^+$], 147.07 [$C_{11}H_{15}^+$], 161.11 [$C_{12}H_{17}^+$], 369.45 [$C_{27}H_{45}^+$], and one mass corresponding to the whole cholesterol molecule m/z 386.37 [$C_{27}H_{46}O^+$]. As shown in Fig. 3 A, in fraction (1) of EVs mixture, statistically significant changes occurred only for two ions with the highest masses. In the subpopulation of ectosomes (Fig. 3 B) statistically significant differences were observed for all characteristic masses with higher mean intensity values for NG conditions. A similar situation occurred for exosomes, except the mass m/z 161.11 [$C_{12}H_{17}^+$], for which no significant change was shown. Our results, seemingly controversial and not as expected, assuming that dyslipidemia is the important risk factor and a hallmark of T2D and metabolic syndrome, give us a new insight into lipid turnover during HG. In the *in vitro* model, cholesterol sulfate, a predominant sterol distributed in biological fluids and tissues, promoted β-cell proliferation and protected them against apoptosis [29].

Multiple studies have shown a link between increased production of superoxide anion (O_2^-), which is one of the reactive oxygen species (ROS) and diabetes. It has also been proven that supplementation with α-tocopherol (vitamin E) reduces the level of ROS [30]. HG-induced increased release of O_2^- is triggered by the activity of protein kinase C (PKC) -α, which, when blocked by tocopherol, inhibits the release of O_2^- [31]. In our study, we observed different intensities of α-tocopherol after glucose stimulation for the ectosome and the exosome (Fig. 3 D, E, F).

For the analysis of α-tocopherol presence four masses corresponding to three fragments: m/z 165.065 [$C_{10}H_{13}O_2$]$^+$, 203.08 [$C_{13}H_{15}O_2$]$^+$, 205.10 [$C_{13}H_{17}O_2$]$^+$ and the molecular ion at m/z 430 [$C_{29}H_{50}O_2$]$^+$ were considered. For fraction (1), a statistically significant change was found only for the highest mass, while the most significant intensities were detected in ectosomes under NG conditions, with exception for the mass corresponding to the molecular ion. As in this case, the HG ectosomes were characterized by the higher intensity and significant changes were observed for two fragments of α-tocopherol.

3.2.4. Glycerolipids

In our study, we analyzed six masses corresponding to monoacylglycerols (MAG), diglycerides (DAG) and triglycerides (TAG)

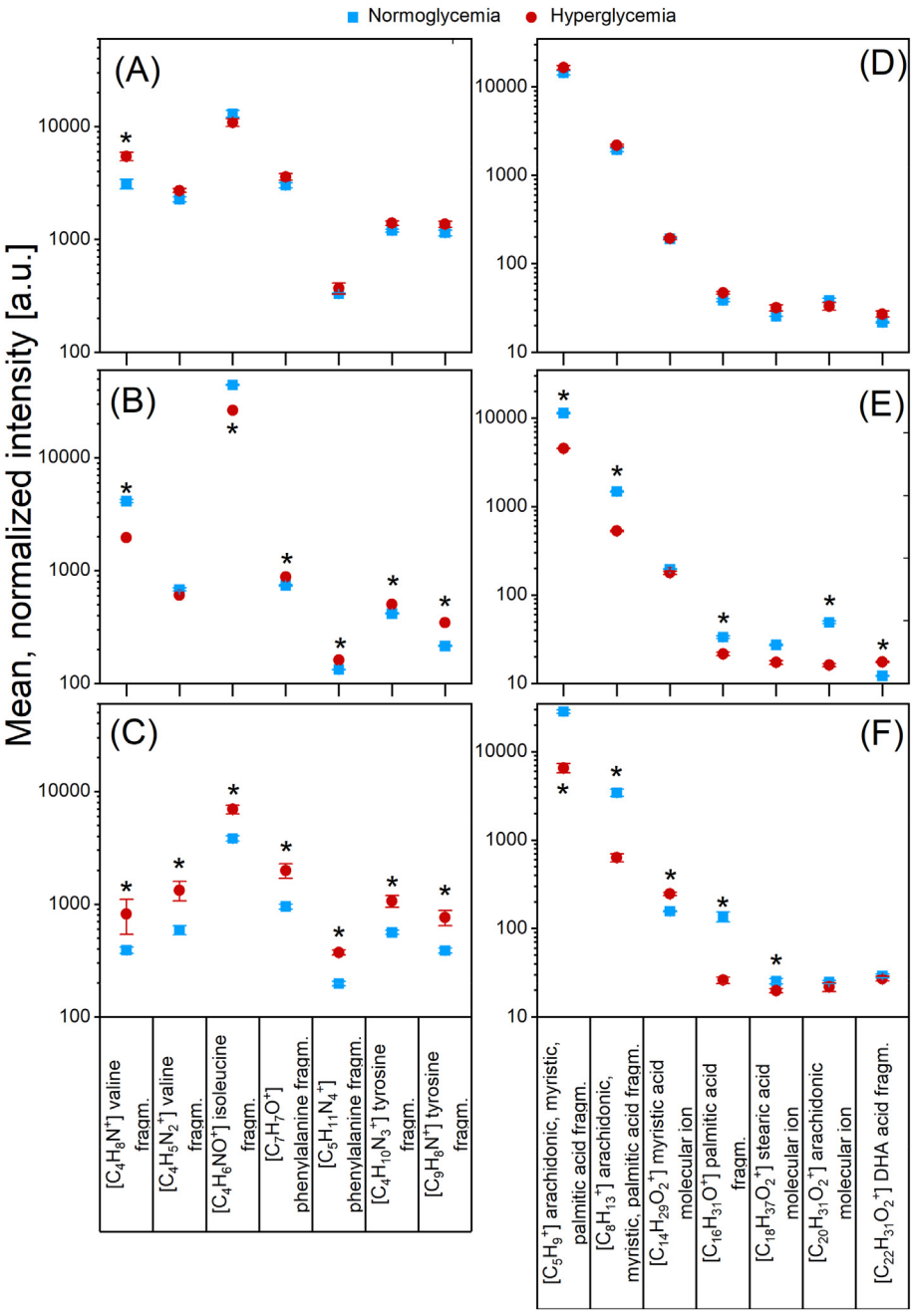

Fig. 2. Mean, normalized ion intensities of the characteristic peaks in positive polarity for amino acids in case of (**A**) mixed EVs, (**B**) ectosomes and (**C**) exosomes; for fatty acids in case of (**D**) mixed EVs, (**E**) ectosomes and (**F**) exosomes. Correlational analysis: *statistically significant with *p*-value <0.05.

(Fig. 4 A, B, C).

No statistically significant changes in the mixed EVs were detected, where in the fraction (2) a significant change were for two masses. Higher mean intensity for HG ectosomes was found for MAG 16:1 (*m/z* 312.17 [$C_{19}H_{35}O_3^+$]). The second mass, for which the change was noted, is characteristic for the TAG 50:0 fragment (*m/z* 833.55) [32]. In this case, the higher intensity is for the NG conditions. In the group of exosomes, significantly higher intensities were determined for NG conditions. The changes concern three masses: *m/z* 567.36; 593.43; 805.57, characteristic for DAG 32:0, DAG 34:1, TAG 48:0 fragments, respectively.

For the analysis of the glycerophospholipid group, seven masses were considered. These are the masses characteristic for the glycerophosphocholine (GPC) fragment (*m/z* 246.12), phosphatidylcholine (PC) 32:0 fragment (*m/z* 478.57), phosphatidylcholine (PC) 28:0 fragments (*m/z* 495.31; 700.52), phosphatidylethanolamine (PE) 28:0 fragment (*m/z* 636.72) and PE 32:0 fragments (*m/z* 692.64; 714.55). In the EV mixture (fraction (1)) only for one mass, characteristic for GPC, a statistically significant change was demonstrated and the higher intensity was observed in NG conditions (Fig. 4 D).

In the group of ectosomes statistically significant changes were observed for all presented masses (Fig. 4 E), but higher intensities were noted for EVs in the HG condition. On the other hand, for the smallest mass, the higher intensity occurred for normoglycemic EVs. In the subpopulation of exosomes statistically significant

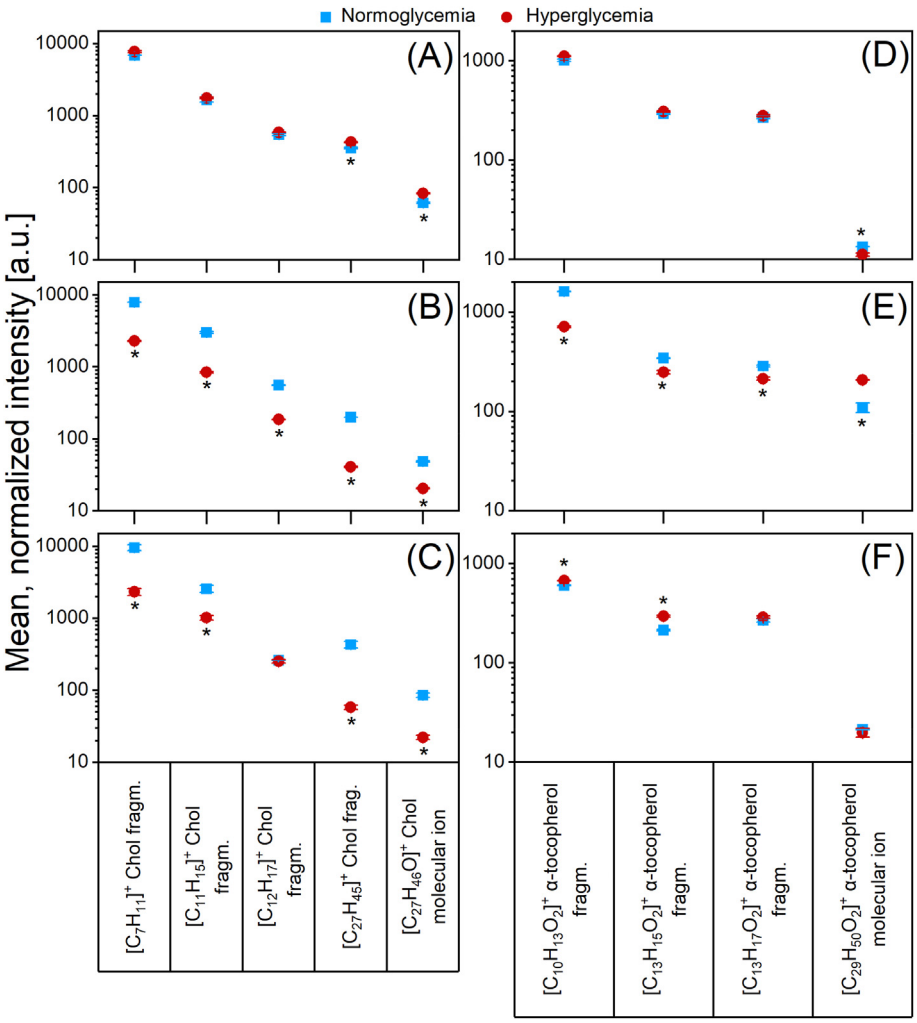

Fig. 3. Mean, normalized ion intensities of selected, characteristic peaks in positive polarization for sterols, where **A**) mixed EVs, **B**) ectosomes, **C**) exosomes; for prenols in case of (**D**) mixed EVs, (**E**) ectosomes, (**F**) exosomes. Correlational analysis: *statistically significant with p-value <0.05.

changes were noted only for two masses (Fig. 4 F). For the first mass, characteristic for the GPC fragment, the higher intensity was noted for HG EVs, while for the second mass, the higher intensity was noted for the NG condition.

3.2.5. Sphingolipids

Five characteristic masses were taken into account for the analysis of sphingolipids: two fragments of phosphosphingolipids, ethanolamine phosphate and two fragments of ceramides (Cer 36: 1) (Fig. 4 G, H, I). In the fraction (1), for one mass, characteristic for ceramide, the statistically significant difference was found between the EVs in HG and the control group (Fig. 4 G). For this mass (m/z 264.30) higher intensity was demonstrated for hyperglycemic EVs. In the case of ectosomes, higher intensity for normoglycemic EVs for all analyzed masses. The opposite tendency was observed for exosomes, where for three smallest masses (m/z 102.10, 104.12, 142.05) significantly higher intensities were obtained for EVs from β-cell culture conditions with increased glucose concentration. For the other two masses, higher mean, normalized intensities were calculated for normoglycemic EVs.

4. Conclusion

This article presents the analysis of the content of selected lipids (including fatty acids, sterols, prenols, glycerolipids and sphingolipids) and amino acids in two subpopulations of EVs derived from pancreatic β-cells stimulated with two glucose concentrations (11 and 35 mM). The analysis of molecular content was carried out based on a comparison of the mean, normalized intensities for the characteristic peaks using the ToF-SIMS technique.

Changes in the molecular content were indicated for AAs such as valine, isoleucine, phenylalanine and tyrosine. This finding confirms that hyperglycemia alters β-cell metabolism, with the significant influence of protein turnover, and confirms previous clinical reports [22,23]. The changes in FA content between different EV fractions were demonstrated, which indicates that both exosomes and ectosomes are rich in lipids, and their molecular content varies with the changes in maternal cell metabolism, what indicates a specific sorting of lipid species in the membrane of EVs. Importantly, our study as the first shows that cholesterol abundance is reduced in hyperglycemic EVs derived from β-cells. This is an important finding, showing that cholesterol metabolism is an important pathway supporting β-cells under hyperglycemic stress [29].

To conclude, the research illustrates the use of an advanced physical technique, ToF-SIMS, to compare EV subpopulations from a β-cell line under specific culture conditions. The use of this technique allows for the gradual acquisition of the missing

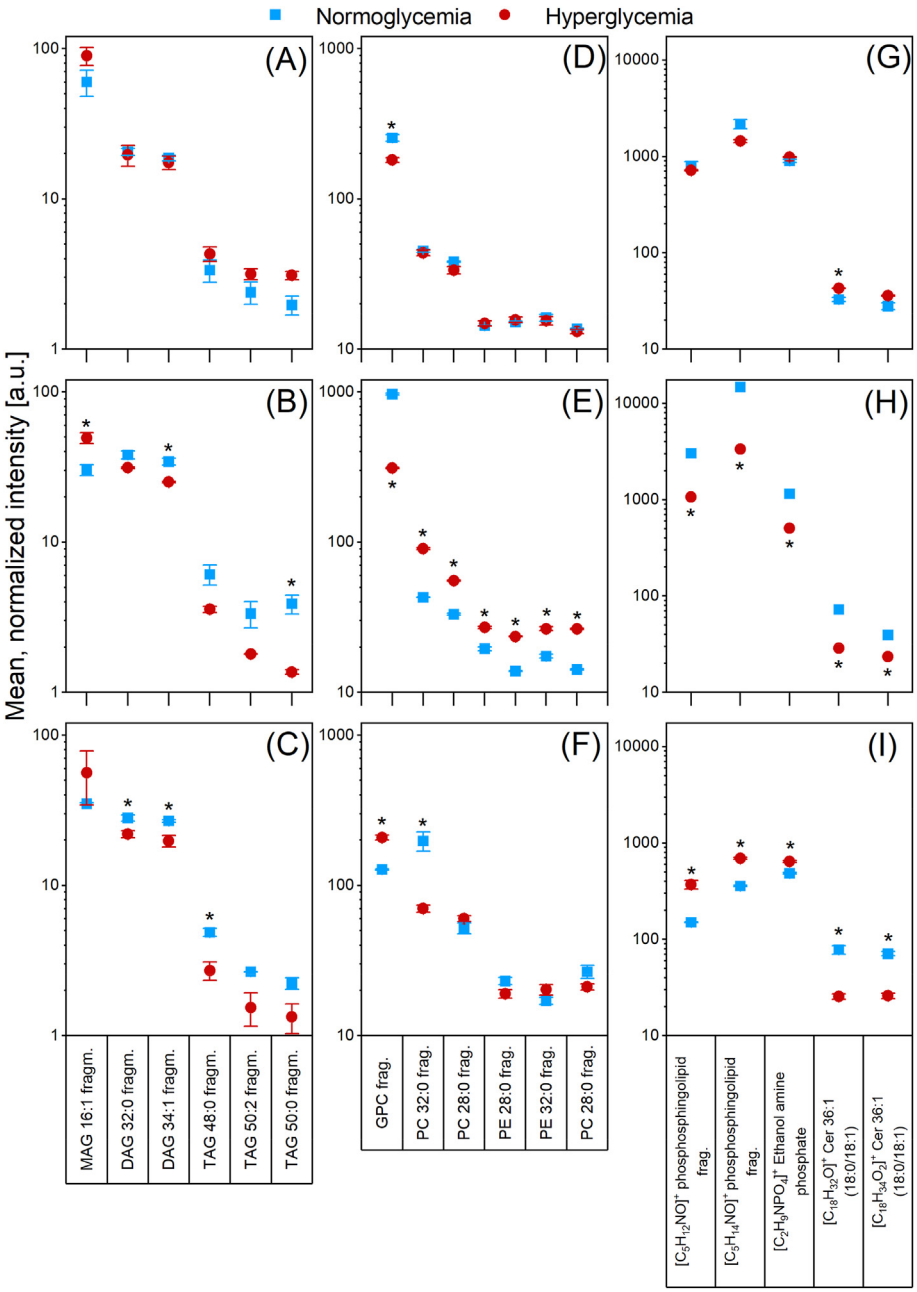

Fig. 4. Mean, normalized ion intensities of selected, characteristic peaks in positive polarization for glycerolipids in case of (**A**) mixed EVs, (**B**) ectosomes, (**C**) exosomes; for glycerophospholipids in case of (**D**) mixed EVs, (**E**) ectosomes, (**F**) exosomes; for glycerolipids in case of (**G**) mixed EVs, (**H**) ectosomes, (**I**) exosomes. Correlational analysis: *statistically significant with p-value <0.05.

knowledge about EV in the field of lipidomic and the functioning of biological systems [2,33].

Data availability

The datasets generated and/or analyzed during the current study are available Marzec, M., Stępień, E., & Rząca, C. (2022). *Testing the influence of hyperglycemia on the content of amino acids, fatty acids and selected lipids in extracellular vesicles using tof-sim.* Repository of the Jagiellonian University. https://doi.org/10.26106/amhp-pm24.

Declaration of competing interest

The authors declare that they have no known competing financial interests or personal relationships that could have appeared to influence the work reported in this paper.

Acknowledgments

1) This publication has been funded from the SciMat and qLife Priority Research Area budget under the Strategic Programme Excellence Initiative at the Jagiellonian University.

2) This work was supported by the National Science Center (NCN), grant OPUS 17 to prof. E. Stępień (No. 2019/33/B/NZ3/

01004).

3) qNano purshase was financed by National Science Center Poland (Grant OPUS 17 No: 2019/33/B/NZ3/01004 to E. Stępień.

Appendix A. Supplementary data

Supplementary data to this article can be found online at https://doi.org/10.1016/j.bbrc.2022.07.020.

References

[1] M.E. Marzec, D. Wojtysiak, K. Połtowicz, J. Nowak, R. Pedrys, Study of cholesterol and vitamin E levels in broiler meat from different feeding regimens by TOF-SIMS, Biointerphases 11 (2016), 02A326, https://doi.org/10.1116/1.4943619.

[2] M.K. Passarelli, N. Winograd, Lipid imaging with time-of-flight secondary ion mass spectrometry (ToF-SIMS), Biochim. Biophys. Acta 1811 (2011) 976–990, https://doi.org/10.1016/j.bbalip.2011.05.007.

[3] A. Kamińska, K. Gajos, O. Woźnicka, A. Dłubacz, M.E. Marzec, A. Budkowski, E. Stępień, Using a lactadherin-immobilized silicon surface for capturing and monitoring plasma microvesicles as a foundation for diagnostic device development, Anal. Bioanal. Chem. 412 (2020) 8093–8106, https://doi.org/10.1007/s00216-020-02938-5.

[4] A. Kamińska, M.E. Marzec, E.Ł. Stępień, Design and optimization of a biosensor surface functionalization to effectively capture urinary extracellular vesicles, Molecules 26 (2021), https://doi.org/10.3390/molecules26164764.

[5] E.Ł. Stępień, C. Rząca, P. Moskal, Novel biomarker and drug delivery systems for theranostics – extracellular vesicles, Bio. Algorithm Med. Syst. 17 (2021) 301–309, https://doi.org/10.1515/bams-2021-0183.

[6] E.R. Abels, X.O. Breakefield, Introduction to extracellular vesicles: biogenesis, RNA cargo selection, content, release, and uptake, Cell. Mol. Neurobiol. 36 (2016) 301–312, https://doi.org/10.1007/s10571-016-0366-z.

[7] E.Ł. Stępień, A. Kamińska, M. Surman, D. Karbowska, A. Wróbel, M. Przybyło, Fourier-Transform InfraRed (FT-IR) spectroscopy to show alterations in molecular composition of EV subpopulations from melanoma cell lines in different malignancy, Biochem. Biophys. Reports. 25 (2021) 100888, https://doi.org/10.1016/j.bbrep.2020.100888.

[8] S. Nomura, Dynamic role of microparticles in type 2 diabetes mellitus, Curr. Diabetes Rev. 5 (2009) 245–251, https://doi.org/10.2174/157339909789804404.

[9] D. Burger, M. Turner, F. Xiao, M.N. Munkonda, S. Akbari, K.D. Burns, High glucose increases the formation and pro-oxidative activity of endothelial microparticles, Diabetologia 60 (2017) 1791–1800, https://doi.org/10.1007/s00125-017-4331-2.

[10] A. Giannella, C.M. Radu, L. Franco, E. Campello, P. Simioni, A. Avogaro, S.V. de Kreutzenberg, G. Ceolotto, Circulating levels and characterization of microparticles in patients with different degrees of glucose tolerance, Cardiovasc. Diabetol. 16 (2017) 118, https://doi.org/10.1186/s12933-017-0600-0.

[11] M.E. Francois, E. Myette-Cote, T.D. Bammert, C. Durrer, H. Neudorf, C.A. DeSouza, J.P. Little, Carbohydrate restriction with postmeal walking effectively mitigates postprandial hyperglycemia and improves endothelial function in type 2 diabetes, Am. J. Physiol. Heart Circ. Physiol. 314 (2018) H105–H113, https://doi.org/10.1152/ajpheart.00524.2017.

[12] S. Vasu, N.H. McClenaghan, J.T. McCluskey, P.R. Flatt, Cellular responses of novel human pancreatic β-cell line, 1.1B4 to hyperglycemia, Islets 5 (2013) 170–177, https://doi.org/10.4161/isl.26184.

[13] J. Liu, X. Sun, F.-L. Zhang, H. Jin, X.-L. Yan, S. Huang, Z.-N. Guo, Y. Yang, Clinical potential of extracellular vesicles in type 2 diabetes, Front. Endocrinol. 11 (2021). https://www.frontiersin.org/article/10.3389/fendo.2020.596811.

[14] J.T. McCluskey, M. Hamid, H. Guo-Parke, N.H. McClenaghan, R. Gomis, P.R. Flatt, Development and functional characterization of insulin-releasing human pancreatic beta cell lines produced by electrofusion, J. Biol. Chem. 286 (2011) 21982–21992, https://doi.org/10.1074/jbc.M111.226795.

[15] M. Marzec, E. Stępień, C. Rząca, Testing the Influence of Hyperglycemia on the Content of Amino Acids, Fatty Acids and Selected Lipids in Extracellular Vesicles Using Tof-Sim, 2022, https://doi.org/10.26106/amhp-pm24.

[16] M. Roman, A. Kamińska, A. Drożdż, M. Platt, M. Kuźniewski, M.T. Małecki, W.M. Kwiatek, C. Paluszkiewicz, E.Ł. Stępień, Raman spectral signatures of urinary extracellular vesicles from diabetic patients and hyperglycemic endothelial cells as potential biomarkers in diabetes, Nanomedicine 17 (2019) 137–149, https://doi.org/10.1016/j.nano.2019.01.011.

[17] M.A. Livshits, E. Khomyakova, E.G. Evtushenko, V.N. Lazarev, N.A. Kulemin, S.E. Semina, E. V Generozov, V.M. Govorun, Isolation of exosomes by differential centrifugation: theoretical analysis of a commonly used protocol, Sci. Rep. 5 (2015), 17319, https://doi.org/10.1038/srep17319.

[18] T.J. Wang, M.G. Larson, R.S. Vasan, S. Cheng, E.P. Rhee, E. McCabe, G.D. Lewis, C.S. Fox, P.F. Jacques, C. Fernandez, C.J. O'Donnell, S.A. Carr, V.K. Mootha, J.C. Florez, A. Souza, O. Melander, C.B. Clish, R.E. Gerszten, Metabolite profiles and the risk of developing diabetes, Nat. Med. 17 (2011) 448–453, https://doi.org/10.1038/nm.2307.

[19] C.R. Anderton, B. Vaezian, K. Lou, J.F. Frisz, M.L. Kraft, Identification of a lipid-related peak set to enhance the interpretation of TOF-SIMS data from model and cellular membranes, Surf. Interface Anal. 44 (2012) 322–333, https://doi.org/10.1002/sia.3806.

[20] D.C. Fernández-Remolar, D. Gómez-Ortiz, P. Malmberg, T. Huang, Y. Shen, A. Anglés, R. Amils, Preservation of underground microbial diversity in ancient subsurface deposits (>6 ma) of the rio tinto basement, Microorganisms 9 (2021), https://doi.org/10.3390/microorganisms9081592.

[21] R.E. Goacher, Y. Mottiar, S.D. Mansfield, ToF-SIMS imaging reveals that p-hydroxybenzoate groups specifically decorate the lignin of fibres in the xylem of poplar and willow, Holzforschung 75 (2021) 452–462, https://doi.org/10.1515/hf-2020-0130.

[22] J. Vangipurapu, A. Stancáková, U. Smith, J. Kuusisto, M. Laakso, Nine amino acids are associated with decreased insulin secretion and elevated glucose levels in a 7.4-year follow-up study of 5,181 Finnish men, Diabetes 68 (2019) 1353–1358, https://doi.org/10.2337/db18-1076.

[23] A. Stancáková, M. Civelek, N.K. Saleem, P. Soininen, A.J. Kangas, H. Cederberg, J. Paananen, J. Pihlajamäki, L.L. Bonnycastle, M.A. Morken, M. Boehnke, P. Pajukanta, A.J. Lusis, F.S. Collins, J. Kuusisto, M. Ala-Korpela, M. Laakso, Hyperglycemia and a common variant of GCKR are associated with the levels of eight amino acids in 9,369 Finnish men, Diabetes 61 (2012) 1895–1902, https://doi.org/10.2337/db11-1378.

[24] P.C. Calder, Functional roles of fatty acids and their effects on human health, JPEN - J. Parenter. Enter. Nutr. 39 (2015) 18S–32S, https://doi.org/10.1177/0148607115595980.

[25] B. Sears, M. Perry, The role of fatty acids in insulin resistance, Lipids Health Dis. 14 (2015) 121, https://doi.org/10.1186/s12944-015-0123-1.

[26] V. Ormazabal, S. Nair, O. Elfeky, C. Aguayo, C. Salomon, F.A. Zuñiga, Association between insulin resistance and the development of cardiovascular disease, Cardiovasc. Diabetol. 17 (2018) 122, https://doi.org/10.1186/s12933-018-0762-4.

[27] G.L. Pearson, N. Mellett, K.Y. Chu, E. Boslem, P.J. Meikle, T.J. Biden, A comprehensive lipidomic screen of pancreatic β-cells using mass spectroscopy defines novel features of glucose-stimulated turnover of neutral lipids, sphingolipids and plasmalogens, Mol. Metabol. 5 (2016) 404–414, https://doi.org/10.1016/j.molmet.2016.04.003.

[28] G. Maulucci, O. Cohen, B. Daniel, C. Ferreri, S. Sasson, The combination of whole cell lipidomics analysis and single cell confocal imaging of fluidity and micropolarity provides insight into stress-induced lipid turnover in subcellular organelles of pancreatic beta cells, Molecules 24 (2019), https://doi.org/10.3390/molecules24203742.

[29] X. Zhang, D. Deng, D. Cui, Y. Liu, S. He, H. Zhang, Y. Xie, X. Yu, S. Yang, Y. Chen, Z. Su, Cholesterol sulfate exerts protective effect on pancreatic β-cells by regulating β-cell mass and insulin secretion, Front. Pharmacol. 13 (2022). https://www.frontiersin.org/article/10.3389/fphar.2022.840406.

[30] S. Devaraj, I. Jialal, Low-density lipoprotein postsecretory modification, monocyte function, and circulating adhesion molecules in type 2 diabetic patients with and without macrovascular complications, Circulation 102 (2000) 191–196, https://doi.org/10.1161/01.CIR.102.2.191.

[31] S.K. Venugopal, S. Devaraj, T. Yang, I. Jialal, α-Tocopherol decreases superoxide anion release in human monocytes under hyperglycemic conditions via inhibition of protein kinase C-α, Diabetes 51 (2002) 3049–3054, https://doi.org/10.2337/diabetes.51.10.3049.

[32] A. Seyer, M. Cantiello, J. Bertrand-Michel, V. Roques, M. Nauze, V. Bézirard, X. Collet, D. Touboul, A. Brunelle, C. Coméra, Lipidomic and spatio-temporal imaging of fat by mass spectrometry in mice duodenum during lipid digestion, PLoS One 8 (2013), e58224, https://doi.org/10.1371/journal.pone.0058224.

[33] K. Gajos, A. Kamińska, K. Awsiuk, A. Bajor, K. Gruszczyński, A. Pawlak, A. Żądło, A. Kowalik, A. Budkowski, E. Stępień, Immobilization and detection of platelet-derived extracellular vesicles on functionalized silicon substrate: cytometric and spectrometric approach, Anal. Bioanal. Chem. (2017), https://doi.org/10.1007/s00216-016-0036-5.